

# A SCALING LAW FOR THE DUST CLOUD IN RF DISCHARGE UNDER MICROGRAVITY CONDITIONS

D. I. Zhukhovitskii,\* V. I. Molotkov, and V. E. Fortov

*Joint Institute of High Temperatures, Russian Academy of Sciences, Izhorskaya 13, Bd. 2, 125412 Moscow, Russia*

(Dated: June 16, 2015)

We employ the approximation of overlapped scattering potentials of charged dust particles exposed to streaming ions to deduce the “equation of state” for a stationary dust cloud in the radio frequency (RF) discharge apart from the void–dust boundary. The obtained equation defines the potential of a dust particle as a function of the ion number density, the mass of a carrier gas atom, and the electron temperature. A scaling law that relates the particle number density to the particle radius and electron temperature in different systems is formulated. Based on the proposed approach the radius of a cavity around a large particle in the bulk of a cloud is estimated. The results of calculation are in a reasonable agreement with the experimental data available in literature.

PACS numbers: 52.27.Lw, 83.10.Rs

## I. INTRODUCTION

Dusty or complex plasma is a low-temperature plasma, which includes dust particles with sizes ranging from 1 to  $10^3 \mu\text{m}$ . Due to the higher electron mobility, particles acquire a considerable electric charge. Thus, a strongly coupled Coulomb system is formed.<sup>1–8</sup> In such a plasma, various collective phenomena at the level of individual particles can be observed. Complex plasmas are usually studied in gas discharges at low pressures, e.g., in the radio frequency (RF) discharges. Under microgravity conditions, a large homogeneous bulk of the complex plasma can be observed. The microgravity conditions are realized either in parabolic flights<sup>9–13</sup> or onboard the International Space Station (ISS).<sup>9,14–18</sup>

In most studies, attention is focused on individual particles injected in plasma, which is a model of the rarefied dust cloud. Elaborate theories model the charge of a particle and its screening by the plasma, elementary processes occurring on the particle surface, interaction between the particles and streams of ions and neutrals associated with the momentum transfer, interaction of particles at large distances etc.<sup>1</sup> At the same time in the dust clouds observed experimentally, dust particles are situated at the distances, which are insufficiently large to neglect collective phenomena that control the particle charging and stability of a dust cloud. The strong interaction between dust particles and their interaction with the ions and electrons result in such a collective phenomenon as the void formation. Formation and stability of the voids were investigated in Refs. 19–29. These studies, however, were aimed at the void–dust boundary, and little attention was paid to the parameters of the bulk of a dust cloud apart from the boundary.

Another manifestation of the collective phenomena in a dust cloud is a spatial distribution of the particles. It was noticed long ago that a dust cloud with an arbitrary particle number density could not be created for the given particle radius. The number of particles injected into the RF discharge plasma influences solely the volume occupied by the dust cloud rather than the particle num-

ber density. In different experiments, the latter seems to scale with the particle radius and electron temperature in some way. This phenomenon is not understood so far.

Some experiments are carried out on an inhomogeneous system consisting of the particles with different diameters. The simplest example of such a system is a large particle surrounded by a dense cloud of smaller particles. Usually, this particle called the projectile moves through the cloud with a supersonic or subsonic velocity. Such projectiles are generated using controlled mechanisms of acceleration<sup>10,30</sup>, or they can appear sporadically.<sup>18,31</sup> A strongly coupled Coulomb system like dust particles in the gas discharge plasma can be represented as a system of the Wigner–Seitz cells with a particle in the center of each cell. According to a natural assumption of the cell quasineutrality and to the proportionality between the particle radius and its charge, the particle diameter must be proportional to the cube of cell radius. Instead, it was observed experimentally that the radius of a cell around a projectile is always noticeably larger than it could be expected from the foregoing considerations. This fact was also not understood as yet.

We propose a model of a dust cloud based on the allowance for a collective interaction between a dense cloud of the dust particles and the streaming ions. As it was noted in an early study,<sup>19</sup> stability of a particle in a dust cloud is provided by the balance between the ion drag force and the electric force generated due to the ambipolar diffusion. We point to the fact that a dust cloud realized in the experiment is so dense that the characteristic impact parameter of the momentum transfer from the ions to a particle is *larger* than the interparticle distance. In other terms, the amount of the moment transfer is restricted by the overlap of scattering potentials of neighboring particles. As a consequence, the drag force turns out to be dependent on the particle number density. With due regard for this fact we construct the “equation of state” for the dust cloud based on the equation of force balance, the equation defining the particle charge, and the overall plasma charge balance (quasineutrality). This equation of state is written in dimensionless quan-

tities reduced to their “critical” values similar to those appearing in the van der Waals equation. Based on this equation, one can calculate the particle number density as a function of the ion number density, the electron temperature, and the mass of a carrier gas atom. The obtained equation makes it possible to formulate a *scaling law* for a homogeneous dust cloud, which states that for the same carrier gas, the ratio of the squared interparticle distance to the product of the particle radius and the electron temperature must be constant in different systems. If the ion number density is sufficiently large, the equation of state has no solutions. Apparently, this is indicative of the existence of the void–dust boundary.

The equation of state allows one to treat the simplest inhomogeneous system, namely, a projectile in the dust cloud. We find the radius of a cavity around the projectile from a balance between the changes of the work against the static pressure of dust particles required to create a cavity and the energy of the electric field induced by the charge of a projectile. The static pressure is calculated from the equation of state of dust particles. The resulting cavity radius proves to be proportional to the square root of the projectile radius rather than to the power of 1/3.

The paper is organized as follows. In Sec. II, the equation of state is deduced for a homogeneous dust cloud. The radius of a cavity around a large particle in such a cloud is estimated in Sec. III. Calculation results are compared with available experimental data in Sec. IV, and the results of this study are summarized in Sec. V.

## II. A STATIONARY HOMOGENEOUS DUST CLOUD

Consider a stationary dust cloud in the RF discharge and formulate the condition of a particle mechanical equilibrium. The stability of such a state will not be tested. Consequently, the condition formulated in what follows may refer both to a stable and to an unstable branch of plasma parameters. Under microgravity conditions, a quiescent dust particle is subject to only two forces, namely, the force acting from the electric field  $F_e = eZ_d E$  and the ion drag force  $F_{id} = \sigma_{\text{eff}} n_i m_i v_{T_i} u_i$ . Here,  $Z_d = (a_d T_e / e^2) \Phi_d$  is the dust particle charge in units of the elementary charge  $e$ ,  $a_d$  is the dust particle radius,  $T_e$  is the electron temperature, for which we use the energy units ( $k_B = 1$ ), and  $\Phi_d = e\varphi_d / T_e$  is the dimensionless potential of a dust particle,  $\varphi_d$  is its potential;  $E$  is the electric field strength,  $\sigma_{\text{eff}}$  is the effective cross section of a collision between the ion and the particle,  $n_i$  is the number density of ions inside the dust cloud,  $m_i$  is the ion mass,  $v_{T_i} = (T_i / m_i)^{1/2}$  is the ion thermal velocity, and  $u_i$  is the ion drift velocity, which is implied to be much smaller than  $v_{T_i}$ . In a real system,  $u_i \sim v_{T_i}$  but the expression for the drag force is too complicated in this case for our purpose to make analytical estimates. Since this general expression shows a regular behavior in the region  $u_i \sim v_{T_i}$ <sup>19</sup>, it will not change our estimations

qualitatively if we use the approximation  $u_i \ll v_{T_i}$ .

The ion drag force arises due to scattering of the streaming ions on dust particles. For an isolated dust particle, the Coulomb cross section of the momentum transfer from an ion to a particle is proportional to  $Z_d^2$  and can be estimated in the order of magnitude as  $(a_d \tau \Phi_d)^2$ , where  $\tau = T_e / T_i$ .<sup>28</sup> For typical parameters of a dust cloud in the RF discharge produced on PK-3 Plus setup,<sup>18</sup>  $\tau \Phi_d \sim 300$ , so that  $\sigma_{\text{eff}}^{1/2}$  exceeds noticeably the average distance between the dust particles characterized by the radius of the Wigner–Seitz cell for dust particles  $r_d = (3/4\pi n_d)^{1/3}$ . Under these conditions, the potentials acting on an ion from the neighboring particles overlap. This situation is typical, e.g., for the dense plasma of alkali metal vapors,<sup>32</sup> where the electron mobility is defined by the overlapped potentials of individual scattering atoms. The overlapping reduces  $\sigma_{\text{eff}}$  dramatically, and it can be estimated as  $C r_d^2$ , where  $C$  is some coefficient. If  $r_d \lesssim \lambda_{D_i}$ , where  $\lambda_{D_i} = (T_i / 4\pi n_i e^2)^{1/2}$  is the ion Debye length, the potential of a particle can be approximated by the unscreened Coulomb potential in the most part of a cell except for the vicinity of its boundary. The quasineutrality of the Wigner–Seitz cell leads to an effective cutoff of the Coulomb potential inside the cell at the distance  $\simeq 0.45 r_d$  (see, e.g., Ref. 33). We will assume that the ion–particle scattering is equivalent to the collisions of the ions against a hard sphere with the radius  $0.45 r_d$ . Then the corresponding drag force can be written as  $F_{id} = (\pi/2) r_d^2 n_i \lambda_{in} e E$ , where it has been taken into account that the ion drift velocity in the electric field  $E$  is  $u_i = (\lambda_{in} / m_i v_{T_i}) e E$ , where  $\lambda_{in}$  is the ion mean free path with respect to the collisions against neutrals.

At the equilibrium,  $F_e = F_{id}$ , and we obtain the force balance equation

$$\frac{\pi}{2} r_d^2 n_i \lambda_{in} = \frac{a_d T_e}{e^2} \Phi_d. \quad (1)$$

The particle potential will be defined using the orbital motion limited (OML) approximation, which proves to be useful in most applications.<sup>34,35</sup> The quantity  $\Phi_d$  is a solution of the equation<sup>1</sup>

$$e^{\Phi_d} (1 + \tau \Phi_d) = \frac{n_e}{n_i} (\tau \mu)^{1/2}, \quad (2)$$

where  $\mu = m_i / m_e$ . Note that  $r_d$  is typically greater or much greater than  $a_d (\tau \Phi_d)^{1/2}$ , which means that the OML approximation is still valid, i.e., the ion flux on a particle is almost the same as for an isolated particle, unless the scattering potentials overlap. This is due to the fact that large impact parameters  $\sim r_d$  contribute appreciably to the total Coulomb moment transfer cross section.

Equations (1) and (2) are completed by the local quasineutrality condition

$$n_i = \frac{a_d T_e}{e^2} \Phi_d n_d + n_e, \quad (3)$$

which is accurate to  $\lambda_{D_e}/L$ , where  $\lambda_{D_e} = (T_e/4\pi n_e e^2)^{1/2}$  is the electron Debye length and  $L$  is the system length scale. We introduce the dimensionless quantities  $n_i^* = (e^2 \lambda_{in}^3 / a_d T_e) n_i$ ,  $n_e^* = (e^2 \lambda_{in}^3 / a_d T_e) n_e$ , and  $n_d^* = (4\pi/3) \lambda_{in}^3 n_d$  to reduce Eqs. (1)–(3) to a transcendental equation with respect to  $\Phi_d$  provided that  $\tau$ ,  $\mu$ , and  $n_i^*$  are treated as parameters

$$\frac{e^{\Phi_d}(1 + \tau\Phi_d)}{\tau^{1/2}\mu^{1/2}} + \frac{3}{8} \left( \frac{\pi n_i^*}{2\Phi_d} \right)^{1/2} = 1. \quad (4)$$

Relation (4) is a scaled ‘‘equation of state’’ for the dust cloud in the RF discharge. It defines the dust particle number density

$$n_d^* = \left( \frac{\pi n_i^*}{2\Phi_d} \right)^{3/2} \quad (5)$$

and the electron number density

$$n_e^* = \frac{e^{\Phi_d}(1 + \tau\Phi_d)}{(\tau\mu)^{1/2}} n_i^*. \quad (6)$$

From Eqs. (4)–(6), it is seen that it is impossible to create a dust cloud with an arbitrary particle number density by a simple addition of the particles to the cloud; instead,  $n_d$  is defined by the system parameters.

Approximate solutions of Eq. (4) can be obtained for the limiting cases  $H \ll 1$  and  $H \gg 1$ , where  $H = |Z_d| n_d / n_e$  is the Havnes parameter.<sup>1</sup> In the first case,  $n_e \simeq n_i$ , and  $\Phi_d = \Phi_0$ , where  $\Phi_0$  is the solution of the equation

$$e^{\Phi_0}(1 + \tau\Phi_0) = (\tau\mu)^{1/2}, \quad (7)$$

and we have

$$n_d^* = \left( \frac{\pi n_i^*}{2\Phi_0} \right)^{3/2}. \quad (8)$$

Here, an approximate solution of Eq. (7) is  $\Phi_0 \simeq (1/2) \ln(\mu/\tau) - 1$ .

If the dust particles number density (8) is sufficiently low so that the condition  $H \ll 1$  is satisfied, one can approximate the spatial ion number density distribution by that in the RF discharge without particles. For the sake of simplicity, we will assume that inside a dust cloud, the overall recombination rate enhanced due to recombination on the particle surface is nearly compensated by the ionization rate inhibited by the reduced electron number density. Then the continuity equation for the ions reads

$$\nabla \cdot (n_i \mathbf{u}_i) = 0. \quad (9)$$

The ion flux velocity can be estimated as  $\mathbf{u}_i = (e\lambda_{in}/m_i v_{Ti}) \mathbf{E}$ , where  $\mathbf{E} = (T_e/e) \nabla \ln n_e \simeq (T_e/e) \nabla \ln n_i$  is the electric field strength, and we arrive at

$$\nabla^2 n_i = 0. \quad (10)$$

Assuming the spherical symmetry of the discharge we obtain

$$n_i(r) = \frac{n_{i0} r_0}{r}, \quad n_{i0} = n_i(r_0), \quad (11)$$

where  $r$  is the radial coordinate.

Consider the opposite case  $H \gg 1$ . Here, the quasineutrality equation (3) is reduced to

$$n_i \simeq |Z_d| n_d = \frac{3}{4\pi} \frac{a_d T_e \Phi_d}{e^2 r_d^3}. \quad (12)$$

It follows from (12) and (1) that  $n_d^* = 512/27$  and

$$\Phi_d \simeq \frac{9\pi}{128} n_i^*. \quad (13)$$

Thus, Eq. (4) may have two solutions that correspond to two branches defining the parameters of a dust cloud. The junction of these branches is similar to the critical point characterized by the critical ion, electron, and dust particle density  $n_{ic}^*$ ,  $n_{ec}^*$ , and  $n_{dc}^*$ , respectively. It is natural to associate this critical point with the void–dust boundary.

Figures 1–4 show solutions of Eq. (4) for the typical parameters  $\tau = 135$  and  $\mu = 7.28 \times 10^4$ . Each dependence has two branches corresponding to a low (blue lines) and a high (red lines) dust number density. Both modes can in principle be observed depending on the RF discharge mode, but the low–density branch is positively most likely to be realized in experiment. It is seen in Fig. 1 that the approximations of the lower branch (8) and of the upper branch  $n_d^* = 512/27$  are in a satisfactory correspondence with the exact solution. The branches of dependence  $n_e^*(n_i^*)$  are shown in Fig. 2. Note that at the upper branch in the vicinity of a critical point, this dependence is decreasing. This means that in this region, the electric field strength  $\mathbf{E} = (T_e/e)(\nabla n_e/n_e)$  changes its sign along with the direction of ion streaming. The possibility of such a peculiarity in the vicinity of the void–dust boundary was noted in Ref. 29. However, this does not affect the force balance equation (1) because it is independent of  $\mathbf{E}$ . The electron number density defines the Havnes parameter (Fig. 3). Along the lower branch sufficiently far from the critical point  $H \ll 1$ , therefore, the effect of a dust cloud on the electron and ion distributions can be neglected. At the critical point, the Havnes parameter reaches its maximum  $H = 4.45$ , so that the effect of dust particles on formation of the void–dust boundary must be significant.

Figure 4 demonstrates that the dependence  $\Phi_d(n_i^*)$  is almost symmetric relative to the axis  $\Phi_d = \Phi_c$ , where  $\Phi_c$  is the critical particle potential. Therefore,  $\Phi_c \simeq \Phi_0/2$ . We substitute this into (4) with due regard for (7) to obtain the estimate

$$n_{ic}^* = \frac{64}{9\pi} \left[ 1 - \frac{1}{2} \left( \frac{\tau\Phi_0^2}{\mu} \right)^{1/4} \right]^2 \Phi_0 \approx \frac{64}{9\pi} \Phi_0, \quad (14)$$

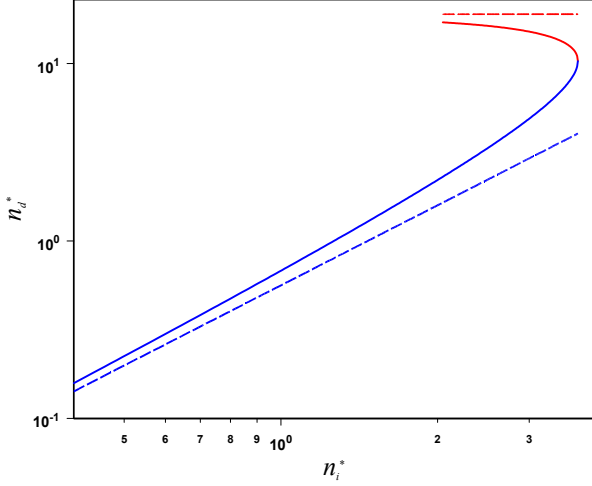


FIG. 1. (Color online) Dust particle number density as a function of the ion number density. Dashed lines indicate approximate solutions for the low-density (8) and the high-density branch  $n_d^* = 512/27$

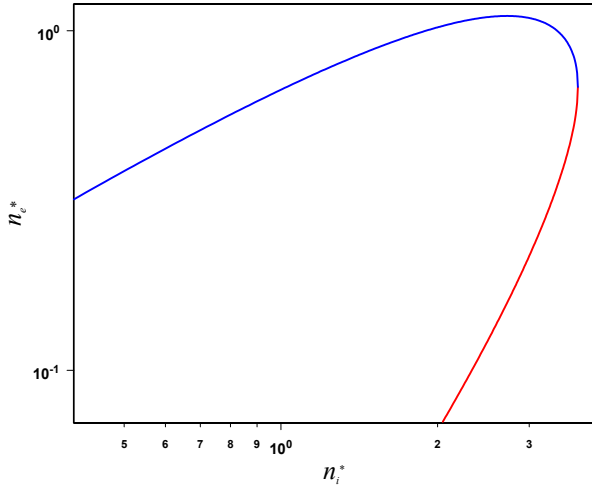


FIG. 2. (Color online) Electron number density as a function of the ion number density

since under typical experimental conditions,  $(\tau\Phi_0^2/\mu)^{1/4}/2 \ll 1$ . We arrive at the conclusion that the critical ion number density  $n_{ic} \approx (64/9\pi)(a_d T_e \Phi_0 / e^2 \lambda_{in}^3)$  is *proportional to the dust particle radius*.

An estimation for the critical electron density follows from (6) with  $\Phi_d = \Phi_0/2$  and (14):

$$n_{ec}^* = \frac{32}{9\pi} \left( \frac{\tau\Phi_0^6}{\mu} \right)^{1/4} \left[ 1 - \frac{1}{2} \left( \frac{\tau\Phi_0^2}{\mu} \right)^{1/4} \right]^2 \quad (15)$$

$$\approx \frac{32}{9\pi} \left( \frac{\tau\Phi_0^6}{\mu} \right)^{1/4}.$$

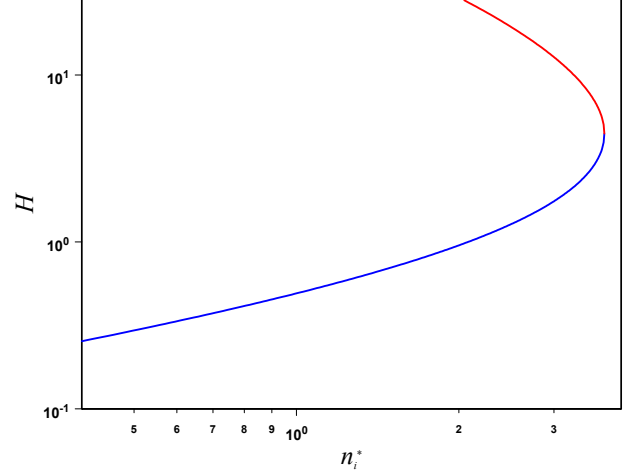


FIG. 3. (Color online) Havnes parameter as a function of the ion number density

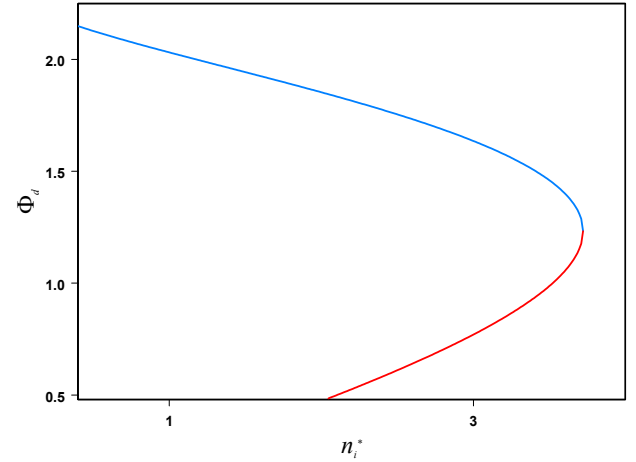


FIG. 4. (Color online) Potential of a dust particle as a function of the ion number density

As is seen in Fig. 1, the upper branch of the dependence  $n_d^*(n_i^*)$  is roughly approximated by a constant  $512/27$ , therefore  $n_{dc}^* \sim 512/27$ , whence it follows that the critical dust number density  $n_{dc} \approx (128/9\pi)\lambda_{in}^{-3}$  is *independent of the dust particle radius*.

We expect  $n_i$  to decrease with the increasing distance from the void center, so that the key assumption of this study,  $a_d \tau \Phi_d \ll r_d$ , flaws at some sufficiently large distance. The limit of validity for the proposed model is defined by the condition  $a_d \tau \Phi_p = (3/4\pi n_d)^{1/3}$ . For the case  $H \ll 1$ , we use (8) and  $\Phi_p \simeq \Phi_0$  to find the lower bound for  $n_i^*$ ,

$$n_i^* = \frac{2}{\pi} \left( \frac{\lambda_{in}}{\tau a_d} \right)^2 \Phi_0^{-1}. \quad (16)$$

Another limitation comes from the Debye screening not taken into account in the foregoing. It was demonstrated<sup>36</sup> that the approximation of the unscreened Coulomb potential results in a correct rate of the momentum transfer between the streaming ions and an *isolated* particle if the ion closest approach to the particle is set to be equal to the ion Debye length. This leads to the maximum impact parameter  $\rho_{\max} = \lambda_{D_i}(1 + 2\Phi_d\tau a/\lambda_{D_i})^{1/2} > \lambda_{D_i}$ . For the Wigner–Seitz cell, the maximum impact parameter is of the order of  $r_d$ . Therefore, the Debye screening can be neglected if  $\rho_{\max} > a_d\tau\Phi_p$ . For typical experimental conditions,  $a \sim 10^{-4}$  cm and the Debye length corresponding to the minimum ion number density is  $\lambda_{D_i} \sim 10^{-2}$  cm (Sec. IV). Thus,  $2\Phi_0\tau a/\lambda_{D_i} > 1$  and  $\rho_{\max} \simeq (2\Phi_d\tau a\lambda_{D_i})^{1/2}$ . With  $n_i^*$  from (16), we have

$$\frac{\rho_{\max}}{a_d\tau\Phi_0} \simeq \left(\frac{\lambda_{in}}{\lambda_{D_i}}\right)^{1/2}. \quad (17)$$

For  $\tau$  and  $\mu$  treated above and  $\lambda_{in} = 2.1 \times 10^{-2}$  cm under experimental conditions, the rhs of Eq. (17) is greater than unity, i.e.,  $\rho_{\max} > r_d$ . This means that the Debye screening can be neglected in this case. However for higher carrier gas pressures, the ratio  $\lambda_{in}/\lambda_{D_i}$  could be less than unity, so that the lower bound for  $n_i^*$  was defined by the Debye screening rather than by the particle potential overlapping. At the same time since  $n_{ic}^*$  (14) is always greater than the minimum ion number density (16), the effect of the Debye screening in the vicinity of a critical point can be neglected in most cases. The range of parameters where the particle potential overlapping dominates is extended if we take into account that in the nonequilibrium gas discharge plasma, the length of Debye screening is larger than  $\lambda_{D_i}$ .<sup>37</sup>

For  $H \gg 1$ , Eq. (13) and the approximation  $n_d^* \simeq 512/27$  yield a lower bound for the high-density branch

$$n_i^* = \frac{16}{3\pi} \frac{\lambda_{in}}{\tau a_d}. \quad (18)$$

The range of parameters in Figs. 1–4 corresponds to the limitations (16) and (18). Since the high-density branch as a whole is not far from the critical point, the Debye screening can be neglected for it as well.

### III. THE RADIUS OF A CAVITY AROUND THE PROJECTILE

Consider a large particle (projectile) with the radius  $a_p$  in a dust cloud of smaller particles. Formation of a cavity around the projectile is quite similar to the cavity formation around a particle, which interacts with the molecules of surrounding liquid via a repulsive potential, known as self-trapping [see, e.g., Ref. 38]. Assuming that the electric field of a charged projectile is screened outside the cavity, we can write the work of formation of a

cavity with the radius  $R_p$  as follows:

$$W(R_p) = \frac{4\pi}{3} p_{st}(R_p^3 - a_p^3) + \frac{Z_p^2 e^2}{2} \left( \frac{1}{R_p} - \frac{1}{a_p} \right), \quad (19)$$

where  $p_{st}$  is the static pressure of the particles in a dust cloud,  $Z_p = (a_p T_e / e^2) \Phi_p$  is the projectile charge, and  $\Phi_p$  is its dimensionless potential. Note that the latter relation implies the neglect of screening of the projectile charge, which is justified in most cases. The first term on the rhs of (19) corresponds to the work against a constant pressure and the second one, to the energy of the electrostatic field induced by the projectile charge. In Eq. (19), we neglect the surface tension term. The equilibrium cavity radius is defined by the condition  $dW/dR_p = 0$ , whence it follows that

$$R_p = \left( \frac{Z_p^2 e^2}{8\pi p_{st}} \right)^{1/4}. \quad (20)$$

Relations like (20) are encountered, e.g., in the theories of positronium self-trapping in liquids.<sup>39</sup> To find  $p_{st}$  we consider the limiting case  $a_p \rightarrow a_d$ . Obviously here  $R_p \rightarrow r_d$ , and the field of a particle is screened inside the Wigner–Seitz cell due to quasineutrality of the latter no matter how small (as compared to the cell radius) the screening length is. Thus, the model equation (20) is still valid in this case, and we readily derive from (1) and (20)

$$p_{st} = \frac{\pi}{32} (en_i \lambda_{in})^2. \quad (21)$$

It is worth mentioning that, as it follows from (20) and the fact that  $Z_p \propto a_p$ , the relation  $R_p \propto a_p^{1/2}$  can be treated as a *scaling law* for a projectile. If the cavity as a whole was neutral (as in a homogeneous system) the scaling would be different:  $R_p \propto a_p^{1/3}$ . Thus for a projectile, we note a violation of the overall quasineutrality of the cell, whose radius is defined by the pressure balance between the cell and surrounding dust cloud. The resulting positive excess charge may break the spherical symmetry of the cell due to the effect of the electric field. This may stipulate the projectile motion. The case of a projectile with a very large radius  $a_p \gg \lambda_{in}$  is treated in Appendix. The only difference from the opposite case  $a_p \ll \lambda_{in}$  treated above is the equation defining the projectile potential (A4). The similarity between (2) and (A4) is indicative of the fact that both cases are qualitatively similar.

### IV. THE ANALYSIS OF AVAILABLE EXPERIMENTS

We start the analysis with the data on the dust clouds formed by particles with the same diameter. It is a special problem, which branch of the solution of Eq. (4)

should be associated with experiment. We suppose that the region far from the critical point along the branch with a high particle number density can hardly be realized under any RF discharge mode because in this case, the rate of the ion–electron recombination on the particle surface would be too high and, due to the low electron number density, the ionization rate would be too low to sustain the discharge. However, this branch can be realized in the vicinity of the critical point in the unstable regime known as the heartbeat oscillations.<sup>40</sup> In any case, the analysis of stability of the high-density branch is a separate problem to be addressed in future. Thus, we confine ourselves with the low-density branch and assume that far apart from the critical point, the effect of dust particles on the ion number density can be neglected.

Since the dust particle number density is usually estimated in the middle of a dust cloud, i.e., far apart from the void–dust boundary or from the critical point, it is reasonable to set approximately  $\Phi_d \simeq \Phi_0$ . Since  $\lambda_{in} \propto 1/p$ , where  $p$  is the pressure of neutral gas atoms, and one can roughly assume that  $n_i \propto p$ ,<sup>41</sup> the product  $n_i \lambda_{in}$  is almost constant. Then it follows from (1) that the ratio

$$\kappa = \frac{r_d^2}{a_d T_e} \quad (22)$$

must assume close values in different experiments. Thus, (22) is a scaling law for different dust clouds in the same carrier gas. Four sets of data of experiments performed in a wide range of argon pressures and particle diameters support this conclusion (Table I):  $\kappa = 0.209 \pm 0.04 \text{ cm/eV}$ .

Since  $Z_d \sim a_d$ , we can deduce from (22) that the maximum impact parameter for the ion–particle collision, which in our model is of the same order as  $r_d$ , must be proportional to  $Z_d^{1/2}$  rather than to  $Z_d$ . The same dependence was obtained in Ref. 36, where the effect of the Debye screening on the ion–particle scattering cross section was investigated for an isolated particle.

We can estimate the ratio  $u_i/v_{T_i}$  for experimental conditions listed in Table I. If we estimate the ion flux velocity as  $u_i = eE\lambda_{in}/m_i v_{T_i}$ , where the electric field strength  $E \simeq T_e/eL$  and  $L$  is the discharge length scale, then  $u_i/v_{T_i} \simeq \tau\lambda_{in}/L$ . Adopting a typical value  $L \sim 1.5 \text{ cm}$  we conclude that the sought ratio is confined in the interval  $0.6 < u_i/v_{T_i} < 1.8$ . This validates our basic relation (1).

Consider the experiments with argon as a carrier gas<sup>18</sup> performed in the PK-3 Plus Laboratory onboard the ISS under microgravity conditions. The details on the setup can be found in Ref. 17. Dust particles injected into the main plasma with dispensers formed a cloud around the center of the chamber. A laser beam expanded to a light sheet was used for visualization of particle positions. Glow of particles illuminated by the laser sheet was recorded using high-resolution cameras, which make it possible to gain the most detailed information concerning a dust cloud. For the gas pressure and temper-

ature of 10 Pa and  $T_n = 300 \text{ K}$ , respectively, we have  $m_i = 6.63 \times 10^{-23} \text{ g}$  and  $v_{T_i} = 2.5 \times 10^4 \text{ cm/s}$ . A dust cloud was formed by the melamine-formaldehyde particles with the radius  $a_d = 1.275 \times 10^{-4} \text{ cm}$  and the mass  $M_d = 1.31 \times 10^{-11} \text{ g}$ .<sup>18,43</sup>

Some larger particles present in the chamber as well get sporadically accelerated and penetrate into the cloud, thus forming projectiles.<sup>19</sup> According to Ref. 43 projectiles are large particles with the radius  $a_p = 7.5 \times 10^{-4} \text{ cm}$ . We can propose the following mechanism of projectile formation. Large particles not evacuated from the chamber after previous experiments are collected in agglomerates containing several particles. Upon illumination by the laser sheet, agglomerated particles are heated and deformed (estimates show that a typical thermal expansion deformations can be of the order of tens of the intermolecular spacing in the particle substance). This deformation is enough to entail cracking of the agglomerates. Then a detached particle is accelerated due to the Coulomb repulsion of the like charges  $Z_p e$ . For a pair of agglomerated particles, the projectile velocity upon penetration into the cloud  $u_p$  can be estimated from the relation  $M_p u_p^2/2 = Z_p^2 e^2/2a_p$ , where  $M_p$  is the projectile mass. With  $Z_p = (a_p T_e/e^2)\Phi_p$ , where  $\Phi_p \approx \Phi_0$ , we arrive at

$$u_p = \frac{T_e \Phi_0}{e} \left( \frac{a_p}{M_p} \right)^{1/2}. \quad (23)$$

For treated experimental conditions,<sup>18</sup> Eq. (23) yields  $u_p \approx 14 \text{ cm/s}$ , which is close to the initial projectile velocity upon penetration into the cloud observed in this experiment. This justifies the proposed mechanism of a projectile acceleration. The collective motion of dust particles induced by the projectile travel through the cloud was studied in Refs. 43–45.

Successive frames of the dust cloud with a projectile moving slowly within it are shown in Fig. 5. A high-resolution camera allows one to resolve the change in the number density of dust particles. As is seen in Fig. 5,  $n_d$  decreases with the increase of the distance from the void center. If we associate  $r_0$  in (11) with the void–dust boundary (a critical point) then  $n_{i0} = n_{ic}$ , and we can use (4), (5), and (11) to calculate the spatial distribution of the particle number density. Calculation result for the particle number density distribution is compared with the data determined from the experiment in Fig. 6. In so doing, the experimental frames presented in Fig. 5 were used for manual determination of  $n_d = \Delta^{-3}$ , where  $\Delta$  is the average visible interparticle spacing. Although this method of the number density determination is used by many authors, an appreciable error may be involved in it. The main sources of this error are unknown type of the crystal lattice and the angles between the vectors of a crystal lattice and the laser sheet plane. Apparently, this method of determination overestimates somewhat  $n_d$ . Nevertheless, Fig. 6 is indicative of a satisfactory agreement between the theory and experiment.

TABLE I. Parameters of the complex plasma in argon RF discharge and the corresponding “dust invariant”  $\kappa = r_d^2/a_d T_e$ .

$p$ , Pa	$2a_d$ , $10^{-4}$ cm	$n_d^{-1/3}$ , $10^{-4}$ cm	$T_e$ , eV	$\kappa$ , cm/eV	Reference
16	1.55	114	3.8	0.170	42
16	2.55	152	3.8	0.184	42
30	9.55	370	4.5	0.245	10
10	2.55	165	3.5	0.235	18

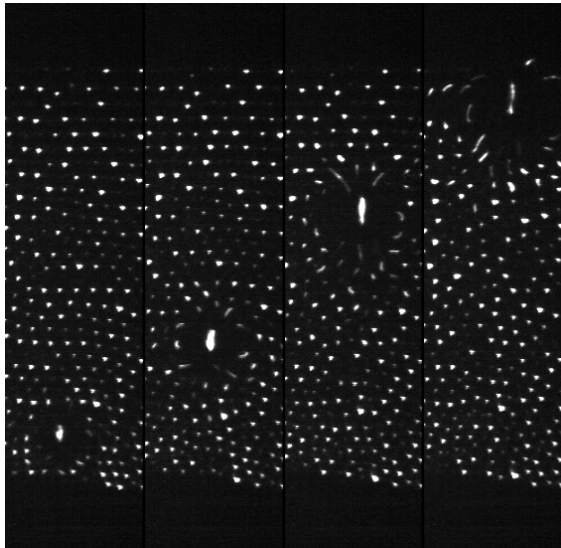
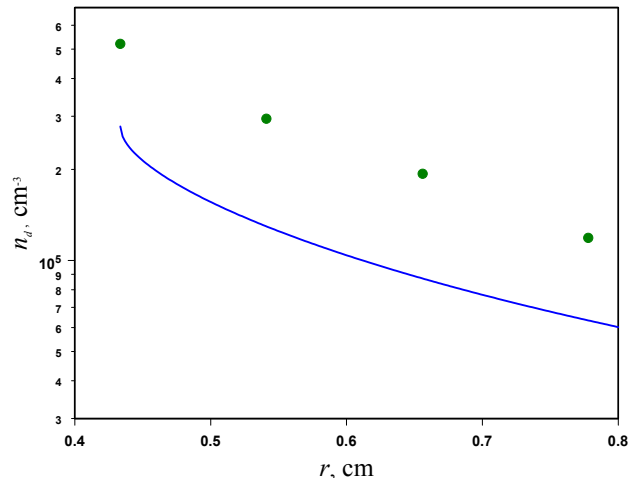
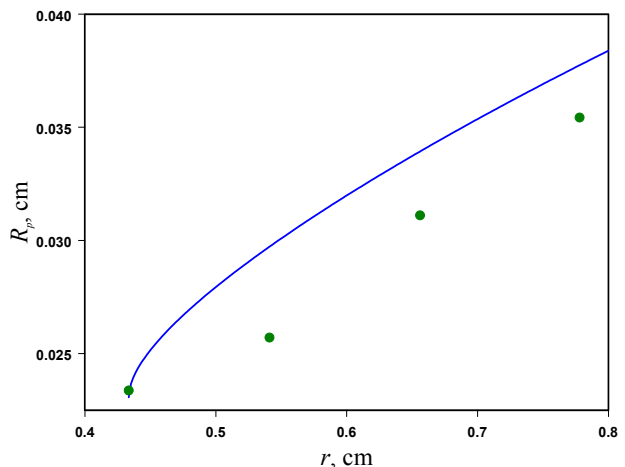


FIG. 5. Snapshots (from left to right) of a projectile moving through the dust cloud in the upward direction toward the electrode, Ref. 18

The distribution of the complex plasma parameters are also illustrated by Figs. 1–4, which correspond to the parameters of the treated experiment. Note that the range of experimental parameters satisfies the condition (16),  $n_d^* > 0.4$ , defining the range of validity for the proposed theory. Also, it is worth mentioning that a rough estimate of the particle number density at the void–dust boundary  $n_{dc} = (128/9\pi)\lambda_{in}^{-3} \approx 4 \times 10^5 \text{ cm}^{-3}$  is close to the experimental value  $5 \times 10^5 \text{ cm}^{-3}$ .<sup>18</sup>

It can be seen in Fig. 5 that the radius of a cavity around the projectile increases with the increase of the distance from the discharge center. This dependence can be determined experimentally by measurement of the cavity radius in the snapshots shown in Fig. 5. Calculation of  $R_p$  can be performed using Eqs. (4), (11), (20), and (21). Figure 7 illustrates a good correspondence between the theory and experiment.<sup>18</sup> According to the estimate (21) the static pressure of dust particles in the middle of a dust cloud is  $p_{st} = 6.3 \times 10^{-7}$  Pa, which correlates with the experimental determination of this quantity at the same point based on the threshold of the projectile cavity deformation ( $p_{st} = 3.0 \times 10^{-7}$  Pa<sup>45</sup>). The obtained value of  $p_{st}$  is in agreement with a theoretical estimate<sup>45</sup>  $p_{st} = Z_p^2 e^2 n_d / 2r_d \approx 5.4 \times 10^{-7}$  Pa as well.

If two types of particles with the radii  $a_1$  and  $a_2$  are

FIG. 6. (Color online) Dust particle number density as a function of the distance from the center of a discharge. Solid line indicates the calculation using Eqs. (4), (5), and (11); dots present processing of the snapshots<sup>18</sup>FIG. 7. (Color online) Radius of a cavity around the projectile as a function of the distance from the center of a discharge. Solid line indicates the theoretical calculation using Eqs. (4), (11), (20), and (21); dots denote processing of the snapshots<sup>18</sup>

injected into the RF discharge then a binary system is formed. We denote the corresponding particle number densities by  $n_1$  and  $n_2$ . Such a system reveals a tendency toward phase separation.<sup>46</sup> At the boundary between two phases, the ion and electron number densities must be continuous. Hence, in the vicinity of a boundary, the potentials of both types of particles must be equal, and we obtain from (1) the scaling law for a binary system

$$\left(\frac{a_1}{a_2}\right)^{1/2} = \left(\frac{n_2}{n_1}\right)^{1/3}. \quad (24)$$

Unfortunately, the accuracy of the available experimental data is insufficient for a direct comparison with the theory.

## V. CONCLUSION

We propose an equation of state for a dense dust cloud in the RF discharge, which expresses the potential of charged particles as a function of the ion number density given the electron temperature and the mass of a carrier gas atom. The key assumption is the overlap of potentials of the dust particles, which scatter streaming ions. As a result, the ion drag force proved to be dependent on the number density of particles. The latter gives rise to a two-branch solution corresponding to the normal and the increased particle number densities. For the branch with a normal density, the equation of state allows one to deduce a scaling law for dust clouds in the RF discharge, which relates the particle number density in a cloud to the particle radius and the electron temperature. As for the branch with the increased density, we expect that its manifestation could be the heartbeat oscillations, while a non-stationary dust cloud is involved in a self-sustained oscillation from one branch to another one. The investigation of stability for both branches will be addressed in future.

A notion of self-trapping of charged particles in condensed matter was used to calculate the radius of a cavity around a large particle (projectile), which penetrates into the dust cloud. The static pressure of dust particles involved in the resulting expression was obtained from the equation of state for a dust cloud. With respect to this problem, the calculation of refined distributions of charged particles within the cell around a projectile would give a clue to understanding the projectile motion through the dust cloud.

A good correspondence with the available experimental data and theoretical estimations of other studies points to the relevance of the proposed approach. Despite this fact, some assumptions involved in the proposed theory are worth discussion. First, the lhs of Eq. (1) utilizes a simplified estimate for the cross section of the momentum transfer from ions to a particle. However, due to the potential overlapping in a dense particle system, refinement of this cross section cannot result in a significant

correction to the results. The correction that is more noticeable could result from taking into account a nonlinear dependence of the drag force on the ion stream velocity in the region  $u_i \sim v_{T_i}$ .

The main objective of the proposed theory is to account for properties of a dust cloud far apart from the void-dust boundary. Nevertheless, it is of interest to extend the theory toward the critical point. In this respect, interpretation of a decreasing dependence of the electron number density on the ion number density in a close vicinity of the critical point (Fig. 2) is an urgent problem. The approximation of the spatial ion density by the dependence (11) in the vicinity of a critical point is knowingly too crude because it does not take into account the difference between  $n_i$  and  $n_e$  at  $H > 1$ . A rigorous approach would imply solution of the Poisson equation instead of the plasma quasineutrality equation (3); the continuity equation (9) should be completed by the ionization and recombination terms. However, complexity of the elementary processes occurring in the gas phase and a deficient information makes a correct simulation of the complex plasma problematic. Another point that is worth a separate treatment is the probable enhancement of the ion flux to the particle surface due to the ion trapping near dust particles and the resulting increase in the frequency of collisions between ions and neutrals. This effect must substantially reduce the particle charge as compared to the OML approximation.<sup>42</sup> We suppose that this problem needs further investigation and can only note that all calculation results discussed in the foregoing are hardly compatible with any approximation other than the OML.

## ACKNOWLEDGMENTS

This research is supported by the Russian Scientific Foundation Grant No. 14-12-01235.

### Appendix A: THE POTENTIAL OF A MACROSCOPIC PARTICLE IN THE PLASMA

We use the model of a cavity around a large particle developed in Sec. III. For a macroscopic particle, however, the OML approximation is invalid because  $a_p \gg \lambda_{in}$ , and we have to estimate the ion flux to the surface of a large particle using an opposite approximation, namely, the diffusion one. We will neglect screening of the particle charge inside the cavity, so that  $Z_p = (a_p T_e / e^2) \Phi_p$ . In this approximation, the ion flux includes the diffusion and drift components,<sup>47</sup>

$$j_+ = -D\nabla n_+ + u_+ n_+, \quad (A1)$$

where  $D \simeq v_{T_i} \lambda_{in}$  is the diffusion coefficient,  $n_+$  is the local ion number density inside the cavity, and  $u_+ \simeq (Z_p e^2 \lambda_{in} / v_{T_i} m_i r^2)$  is its local drift velocity at the distance  $r$  from the cavity center. We substitute (A1) into

the local stationary continuity equation  $\text{div} j_+ = 0$  to derive

$$\frac{d}{d\tilde{r}} \left( \tilde{r}^2 \frac{dn_+}{d\tilde{r}} + n_+ \right) = 0, \quad (\text{A2})$$

where  $\tilde{r} = r/a_p \tau \Phi_p$ . The solution of Eq. (A2) with the obvious boundary conditions  $n_+(a_p) = 0$  and  $n_+(\infty) = n_i$  is

$$n_+(\tilde{r}) = \frac{n_i}{1 - e^{\tau \Phi_p}} \left( e^{\tilde{r}^{-1}} - e^{\tau \Phi_p} \right). \quad (\text{A3})$$

Therefore, the ion flux on the particle surface is  $j_+(a_p) = v_{T_i} \lambda_{in} n_i \tau \Phi_p / a_p$ . It proves to be not much different

from that given by the OML approximation. Indeed, the collisions with neutrals slow down the ions but they remove the energy and momentum limitations on the ions involved in the OML. These two factors seem to attenuate each other. Assuming the Boltzmann distribution for the electrons, we write the electron flux as  $j_-(a_p) = (2\pi)^{-1/2} n_e v_{T_e} \exp(-Z_p e^2 / a_p T_e)$ . In a stationary state,  $j_+(a_p) = j_-(a_p)$ , therefore,  $\Phi_p$  is defined by the equation

$$\Phi_p e^{\Phi_p} = \left( \frac{\mu}{2\pi\tau} \right)^{1/2} \frac{a_p n_e}{\lambda_{in} n_i}. \quad (\text{A4})$$

Combination of (A4), (20), and (21) makes it possible to estimate the radius of a cavity around a macroscopic particle in a dust cloud.

- 
- \* [dmr@ihed.ras.ru](mailto:dmr@ihed.ras.ru)
- <sup>1</sup> V. E. Fortov and G. E. Morfill, eds., *Complex and Dusty Plasmas: From Laboratory to Space*, Series in Plasma Physics (CRC Press, 2009).
  - <sup>2</sup> J. H. Chu and L. I, Phys. Rev. Lett. **72**, 4009 (1994).
  - <sup>3</sup> H. Thomas, G. E. Morfill, V. Demmel, J. Goree, B. Feuerbacher, and D. Möhlmann, Phys. Rev. Lett. **73**, 652 (1994).
  - <sup>4</sup> Y. Hayashi and S. Tashibana, Jpn. J. Appl. Phys. **33**, L804 (1994).
  - <sup>5</sup> S. V. Vladimirov, K. Ostrikov, and A. A. Samarian, *Physics and applications of complex plasmas* (Imperial College, London, 2005).
  - <sup>6</sup> V. Fortov, A. Ivlev, S. Khrapak, A. Khrapak, and G. Morfill, Phys. Rep. **421**, 1 (2005).
  - <sup>7</sup> P. K. Shukla and B. Eliasson, Rev. Mod. Phys. **81**, 25 (2009).
  - <sup>8</sup> M. Bonitz, C. Henning, and D. Block, Rep. Prog. Phys. **73**, 066501 (2010).
  - <sup>9</sup> G. E. Morfill, U. Konopka, M. Kretschmer, M. Rubin-Zuzic, H. M. Thomas, S. K. Zhdanov, and V. Tsytovich, New J. Phys. **8**, 7 (2006).
  - <sup>10</sup> D. Caliebe, O. Arp, and A. Piel, Phys. of Plasmas **18**, 073702 (2011).
  - <sup>11</sup> A. Piel, O. Arp, M. Klindworth, and A. Melzer, Phys. Rev. E **77**, 026407 (2008).
  - <sup>12</sup> K. O. Menzel, O. Arp, and A. Piel, Phys. Rev. E **83**, 016402 (2011).
  - <sup>13</sup> O. Arp, D. Caliebe, and A. Piel, Phys. Rev. E **83**, 066404 (2011).
  - <sup>14</sup> M. Schwabe, S. K. Zhdanov, H. M. Thomas, A. V. Ivlev, M. Rubin-Zuzic, G. E. Morfill, V. I. Molotkov, A. M. Lipaev, V. E. Fortov, and T. Reiter, New J. Phys. **10**, 033037 (2008).
  - <sup>15</sup> G. E. Morfill, H. M. Thomas, U. Konopka, H. Rothermel, M. Zuzic, A. Ivlev, and J. Goree, Phys. Rev. Lett. **83**, 1598 (1999).
  - <sup>16</sup> S. A. Khrapak, B. A. Klumov, P. Huber, V. I. Molotkov, A. M. Lipaev, V. N. Naumkin, H. M. Thomas, A. V. Ivlev, G. E. Morfill, O. F. Petrov, V. E. Fortov, Y. Malentschenko, and S. Volkov, Phys. Rev. Lett. **106**, 205001 (2011).
  - <sup>17</sup> H. M. Thomas, G. E. Morfill, V. E. Fortov, A. V. Ivlev, V. I. Molotkov, A. M. Lipaev, T. Hagl, H. Rothermel, S. A. Khrapak, R. K. Suetterlin, M. Rubin-Zuzic, O. F. Petrov, V. I. Tokarev, and S. K. Krikalev, New J. Phys. **10**, 033036 (2008).
  - <sup>18</sup> M. Schwabe, K. Jiang, S. Zhdanov, T. Hagl, P. Huber, A. V. Ivlev, A. M. Lipaev, V. I. Molotkov, V. N. Naumkin, K. R. Sütterlin, H. M. Thomas, V. E. Fortov, G. E. Morfill, A. Skvortsov, and S. Volkov, EPL **96**, 55001 (2011).
  - <sup>19</sup> J. Goree, G. E. Morfill, V. N. Tsytovich, and S. V. Vladimirov, Phys. Rev. E **59**, 7055 (1999).
  - <sup>20</sup> V. N. Tsytovich, Phys. Scripta **T89**, 89 (2001).
  - <sup>21</sup> V. N. Tsytovich, S. V. Vladimirov, G. E. Morfill, and J. Goree, Phys. Rev. E **63**, 056609 (2001).
  - <sup>22</sup> V. N. Tsytovich, S. V. Vladimirov, and G. E. Morfill, Phys. Rev. E **70**, 066408 (2004).
  - <sup>23</sup> S. V. Vladimirov, V. N. Tsytovich, and G. E. Morfill, Phys. Plasmas **12**, 052117 (2005).
  - <sup>24</sup> M. R. Akdim and W. J. Goedheer, Phys. Rev. E **65**, 015401(R) (2001).
  - <sup>25</sup> V. Land and W. J. Goedheer, New J. Phys. **9**, 246 (2007).
  - <sup>26</sup> W. J. Goedheer and V. Land, Plasma Phys. Control. Fusion **50**, 124022 (2008).
  - <sup>27</sup> K. Avinash, A. Bhattacharjee, and S. Hu, Phys. Rev. Lett. **90**, 075001 (2003).
  - <sup>28</sup> E. Nebbat, R. Annou, and R. Bharuthram, Phys. Plasmas **14**, 093702 (2007).
  - <sup>29</sup> G. Gozadinos, A. V. Ivlev, and J. P. Boeuf, New J. Phys. **5**, 32 (2003).
  - <sup>30</sup> M.-C. Chang, Y.-P. Tseng, and L. I, Phys. of Plasmas **18**, 033704 (2011).
  - <sup>31</sup> D. Samsonov, J. Goree, H. M. Thomas, and G. E. Morfill, Phys. Rev. E **61**, 5557 (2000).
  - <sup>32</sup> D. I. Zhukhovitskii, High Temperature **31**, 36 (1993).
  - <sup>33</sup> D. I. Zhukhovitskii, A. G. Khrapak, and I. T. Yakubov, in *Plasma Chemistry* (Energoizdat, Moscow, 1984), vol. 11, p. 130.
  - <sup>34</sup> H. M. Mott-Smith and I. Langmuir, Phys. Rev. **28**, 727 (1926).
  - <sup>35</sup> J. E. Allen, Phys. Scr. **45**, 497 (1992).
  - <sup>36</sup> S. A. Khrapak, A. V. Ivlev, G. E. Morfill, and H. M. Thomas, Phys. Rev. E **66**, 046414 (2002).

- <sup>37</sup> J. E. Daugherty, R. K. Porteous, M. D. Kilgore, and D. B. Graves, *J. Appl. Phys.* **72**, 3934 (1992).
- <sup>38</sup> T. Mukherjee, B. N. Ganguly, and B. Dutta-Roy, *J. Chem. Phys.* **107**, 7467 (1997).
- <sup>39</sup> D. I. Zhukhovitskii, *Coll. J.* **67**, 718 (2005).
- <sup>40</sup> R. J. Heidemann, L. Couédel, S. K. Zhdanov, K. R. Sütterlin, M. Schwabe, H. M. Thomas, A. V. Ivlev, T. Hagl, G. E. Morfill, V. E. Fortov, V. I. Molotkov, O. F. Petrov, A. I. Lipaev, V. Tokarev, T. Reiter, and P. Vinogradov, *Phys. Plasmas* **18**, 053701 (2011).
- <sup>41</sup> M. Klindworth, O. Arp, and A. Piel, *J. Phys. D: Appl. Phys.* **39**, 1095 (2006).
- <sup>42</sup> S. A. Khrapak, B. A. Klumov, P. Huber, V. I. Molotkov, A. M. Lipaev, V. N. Naumkin, A. V. Ivlev, H. M. Thomas, M. Schwabe, G. E. Morfill, O. F. Petrov, V. E. Fortov, Y. Malentschenko, and S. Volkov, *Phys. Rev. E* **85**, 066407 (2012).
- <sup>43</sup> D. I. Zhukhovitskii, V. E. Fortov, V. I. Molotkov, A. M. Lipaev, V. N. Naumkin, H. M. Thomas, A. V. Ivlev, M. Schwabe, and G. E. Morfill, *Phys. Rev. E* **86**, 016401 (2012).
- <sup>44</sup> A. V. Ivlev and D. I. Zhukhovitskii, *Phys. Plasmas* **19**, 093703 (2012).
- <sup>45</sup> D. I. Zhukhovitskii, A. V. Ivlev, V. E. Fortov, and G. E. Morfill, *Phys. Rev. E* **87**, 063108 (2013).
- <sup>46</sup> G. E. Morfill, A. V. Ivlev, and H. M. Thomas, *Phys. Plasmas* **19**, 055402 (2012).
- <sup>47</sup> P. M. Chung, L. Talbot, and K. J. Touryan, *Electric Probes in Stationary and Flowing Plasmas: Theory and Application* (Springer-Verlag, New York, 1975).